JMRA
Journal of Mechanical Research and Application
ISSN: 2251-7383, eISSN: 2251-7391

Semi-Active Suspension Control Based on Bingham Modified Model Using Prototyped Twin-Tube MR Damper

S. Hamid Mousavi[1*]

1*. Department of Mechanical Engineering, Faculty of Enghelab, Technical and Vocational University Tehran, Iran
(Email: hmousavi@tvu.ac.ir)

Received: 2020-04-22 **Accepted**: 2020-05-11

Abstract: In this article, the prototyped magnetorheological (MR) damper with internal solenoid based on Bingham modified model of MR damper is presented and experimentally tested on a real passenger car. The rolling-lobe type of the existing air spring was replaced with a cylinder-tube type and it was integrated with the MR dampers in order to save the mounting space. The forces generated by the semi-active dampers during valve operation are also measured. In this paper, to use Bingham modified model, an eleven degrees of freedom (DOFs) suspension system (four for four wheels, three for the body displacement and its rotations and the last four for passengers) has been modeled. The results of experiment are analyzed for comfortable driving and road holding. Comparisons between the results from the vehicle model and the experimental were good and acceptable. The most important features of the fabricated MR damper are low cost of production and simple structure.

Keywords: Bingham model, MR damper, Suspension system

1. Introduction

In car industries, suspension systems are of tremendous importance. It handles multiple tasks such as keeping the contact between vehicle tires and the road, dealing with the stability of the vehicle, and separating the frame of the vehicle from road made vibration and shocks. Generally, ride comfort, road handling, and stability are the key factors to assess suspension performance. In the current paper, the amplitude of the car vibration caused by applied road profile is decreased by modifying passenger car's suspension system.

In the passive suspension system, the stiffness and damping parameters are stable and it is believed that applying semi-active suspension systems adapted to varied road conditions using an actuator could tackle this problem; consequently, MR dampers are added to the typical suspension systems whereas the other parts of suspension system remain unchanged. The key feature of MR damper is the ability to change its viscosity by varying magnetic field.

By implanting half car model, Parabakar et al. [1] simulated semi-active suspension system. They modified Bouc-Wen model and determined them for fitting the hysteretic behavior to model MR damper. Yahaya et al. [2] investigated vibration control of a passenger car using half car.

Zareh et al. [3] modeled the vehicle suspension system by full car model for enhancing the accuracy of car model. They were able to enhance the accuracy of model component to quarter car and half car models. Dong et al. [4] discuss the rapid control prototyping approach used for development and investigation of control algorithm in magnetorheological (MR) semi-active suspension system. Nell et al. [5] assessed an unsophisticated two state semi-active damper experimentally; however, they did not focus on variable fluid compressibility. Elmer et al. [6] studied more complex model of hydraulic control valves including variable coil inductance and valve spool dynamics. Jazar et al. [7] developed an industrial application of MR fluids. Eslaminasab et al. [8] suggested in-house semi-active damper with actuated valve for heavy vehicles. They considered the effect of bulk modulus on the behavior of fluid compression. Zapateiro et al. [9] simulated two control methodologies used to design semi active controllers for suspension systems that make use of magnetorheological dampers. The first methodology is based on the back stepping technique and the second one is the quantitative feedback theory.

Leading automotive companies such as General Motors and Volvo have started to use the semi-active actuators in the suspension systems of high-end automobiles, such as the Cadillac Seville and Corvette, to improve the handling and ride performance in the vehicles. Nevertheless, much more researches and developments are needed in commercial design, fabrication, and control of semi-active suspension systems. To achieve this objective, development of an experimental simulation system for real-time control of an experimental test bed is considered; therefore, an in-house semi-active twin-tube shock absorber with an internal variable solenoid-actuated will be prototyped. The main aim of this research is to show that the prototyped MR damper is implementable with low cost of production has ability to implement on real common passenger vehicles.

2. Car model

In this model, all wheels and passengers rely on each other and on the car body in the full-car model. It is believed that each wheel affects the spring and the damper of other wheels, and there is a link between the two axes of the vehicle [3]. The effect of road profile on the passengers is dampened using MR actuator. It worth noting that the MR shock absorber is added to the axel and the car body. In the full-car model, the effect of body rotations around roll and the yaw axis is exerted through simulation [10]. The suspension system using the full-car model is consisted of 11-DOFs, of which four are for the four wheels, three for the body displacement and its rotations and the last four for passengers. Figure 1 shows the schematic of the full-car model with 11-DOFs and an added MR damper is shown [10].

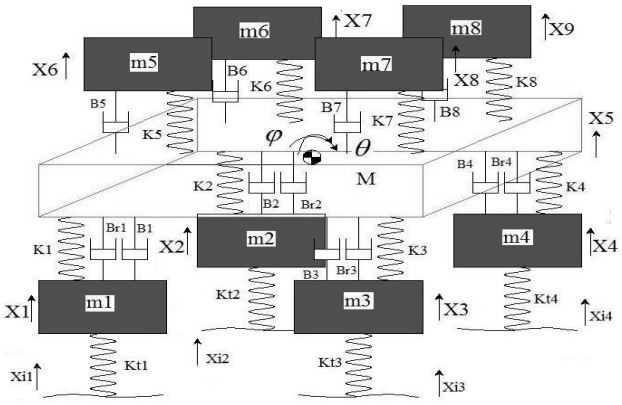

Figure 1) Car model with eleven degrees of freedom.

where M_b and m_{1-8} represent masses of body, wheels and passengers. The terms k_{1-8} and b_{1-8} represent stiffness and damping coefficients of the model, respectively. The terms k_{t1}, k_{t2}, k_{t3} and k_{t4} are stiffness of the tires. The terms x_{i1}, x_{i2}, x_{i3} and x_{i4} indicate load profile. More detailed explanations and dimensions about the full car model are available in [3,10]; so to avoid a lengthy discussion and save page number, the details are not express here.

3. Prototyped MR damper

Unfortunately, no commercially available damper has been found for the common passenger automobiles, thus luxury passenger vehicle applications have been earlier tested by adopting and manufacturing of MR dampers. Nevertheless, because of amount of required MR-fluid for a common passenger automobile damper and the cost of MR-fluids, available MR dampers did not fit [8]. For this aim, an internal solenoid structure is suitable for our objective because of its cost and force-velocity characteristic due to its cost-effective (required less MR-fluid) and easy-to-implement solutions. For an optimal design of the piston value, it is necessary to secure B-H curve data. The MR fluid used in this study is MRF-140CG of the LORD Corporation. Figure 2 shows the shear curve for the MRF and magnetic circuit.

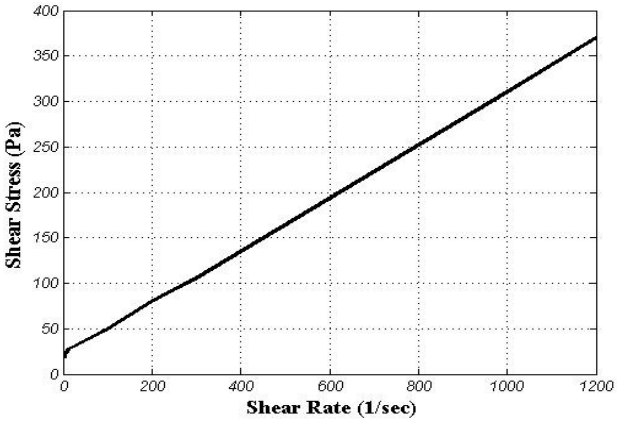

Figure 2) The shear curve of the MRF-140CG.

The final objective of the modeling addressed here is finding a parametric relation between damper velocity and the solenoid voltage to the damping force to easily analyze the performance of the damper and fine-tune different parameters and parts (such as orifice size or solenoid force). The model is separated in two parts for simplifying the modeling process. In first, the fluid flow and pressure balance equations for the damper piston are determined. The second part deals with the modeling of the solenoid and the internal valve system inside the piston. The free-body diagram of the piston and the applied forces due to the damper movements because of an external force (F_{damper}) and generated pressure difference are depicted in Figure. 3. The equation for the piston's motion is:

$$F_{damper} = F_{compression} - F_{extension} + F_{friction} + M_d \ddot{x} \quad (1)$$

where the compression chamber force ($F_{compression}$) is:

$$F_{compression} = P_c A_P = P_c \pi R_P^2. \quad (2)$$

where P_c is the compression chamber pressure, A_P is the piston area, and R_P is the piston internal radius. The extension chamber force ($F_{extension}$) is:

$$F_{extension} = P_E(A_P - A_R) = P_E(\pi R_P^2 - \pi R_R^2) \tag{3}$$

where P_E is the extension chamber pressure, A_R is the piston rod area, and R_R is the piston rod radius. Note that both P_E and P_c are gauge pressures. The friction force ($F_{friction}$) in current study is assumed constant with the magnitude of F_f.

$$F_{friction} = F_f\left(\frac{|\dot{x}|}{\dot{x}}\right) \tag{4}$$

Therefore, Eq. (1) is re-written as:

$$F_{damper} = P_c\pi R_P^2 - P_E(\pi R_P^2 - \pi R_R^2) + F_f\left(\frac{|\dot{x}|}{\dot{x}}\right) + M_d\ddot{x} \tag{5}$$

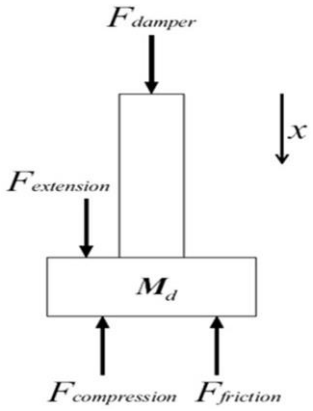

Figure 3) Schematics of the piston [8].

For predicting the damping force from this equation, the pressure in the compression and extension cases (P_c and P_E). The free-body diagram of the valve disc and the applied forces are depicted in Figure. 4. The major forces on the disc are:

1) Pressure force ($F_{pressure}$) because of the pressure difference made by piston motion.

2) Fluid flow force ($F_{fluidflow}$) because of the fluid direction changes, thus, variations of fluid momentum.

3) Spring force (F_{spring}) because of the existence of balancing springs.

4) Force generated by solenoid ($F_{solenoid}$) because of the existence of push type solenoid.

$$F_{spring} + F_{solenoid} - F_{fluidflow} - F_{pressure} + M_v\ddot{x} = 0 \tag{6}$$

Q_{TV} is the total valve flow and is proportional to the damper velocity with the following equation:

$$Q_{TV} = \dot{x}(\pi R_P^2 - \pi R_R^2) \tag{7}$$

The fluid force ($F_{fluidflow}$) is generated because of the change in the direction of fluid flow as well as the change of momentum. The magnitude of this force is calculated using the following equation:

$$F_{fluidflow} = \rho Q_{TV} v_{Fluid}\cos(\theta_f). \tag{8}$$

where the angle θ_f is the change in fluid direction, which is considered 69° for the regular orifice [17]. For the internal valve, and because of the many uncertainties about the fluid characteristics, the fluid force is supposed insignificant and ignored the equations. The spring force (F_{spring}) is modeled as a linear force producing a force relative to the valve displacement.

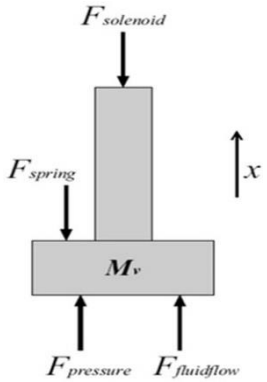

Figure 4) Valve disc free-body diagram [8].

$$F_{spring} = k_v x \tag{9}$$

where k_v is the valve spring stiffness. The stiffness of the spring applied in the valve is variable, and it must be chosen according to the valve modeling and the valve geometry. The force made by solenoid ($F_{solenoid}$) is a function of selected solenoid for this application and is provided by the solenoid manufacturer; choosing a suitable solenoid for this application is one of the key objectives of for simulation and modeling. Table 1 depicts the estimated model parameters of the MR damper modeled with a friction component amplified by a Newtonian viscosity component. In contrast, the modeling and simulation aims at determining a few of the unidentified parameters of the system by trial and error method. Such parameters are included the solenoid.

Table 1. Physical parameters of the new MR damper

Symbol	Description	Value
Ap	Piston area (m^2)	0.0008
A_R	Piston rod area (m^2)	0.00021
Rp	Piston internal radius (m)	0.016
R_R	Piston rod radius (m)	0.0098
Md	Piston and rod mass (kg)	3.1
Mv	Valve disc and valve shaft mass (kg)	0.75
ρ	Fluid density (kg/m^3)	3540
L	Length of the piston (m)	0.055
D_h	Diameter of small orifices in the piston (m)	0.002

The generated force by applied solenoid is expressed by:

$$F_{solenoid} = \frac{B_{gap}^2 A_{gap}}{2\mu_0} \tag{10}$$

where B_{gap} and A_{gap} is the flux density and air gap area, respectively. Using of $B=NI/R_{mag}A$ [18], where I is the input current, the force of solenoid is modified to:

$$F_{solenoid} = \frac{N^2 I^2}{2R_{gap} A_{gap} \mu_0} \tag{11}$$

The drop-off rate of the force drop is dependent on the dimension, material and its plunger form. Here, the design objective is the valve spring using of linear spring model for countering the drop-off. The solenoid model which is selected in this study is S-22-150-HF. The force vs. displacement graph for the solenoid and spring (spring rate=204 kN/m) is shown in Figure. 5.

As Figure. 6 shows, an air spring consists of six parts including the upper cap, upper sealing part, air spring piston, inner tube, outer tube, and lower sealing part. All the parts other than the cylinder tube can be used as both front and rear parts. The air spring piston is installed on the upper end of the MR damper and it fixes the rod guide of the MR damper. It performs the function of the piston, which changes the volume and pressure of the cylinder tube, and at the same time, it carries out the role of sealing which maintains pressure by preventing the internal nitrogen gas from leaking. The inner tube changes the spring load by changing the volume and plays the role of the accumulator together with the outer tube. The inner tube and outer tube have different lengths but other dimensions are all the same.

The cross section of the twin-tube damper is shown in Figure. 6(a). The compression chamber is separated from the reservoir chamber by foot valve. The donut seals do not allow the oil to mix with the gas. The gas pressure is provided by a valve which is installed on the gas case. Two poppets are used as the foot valve for compression and rebound. The fluid in compression condition passes through holes of piston 8 (Figure. 6(b)).

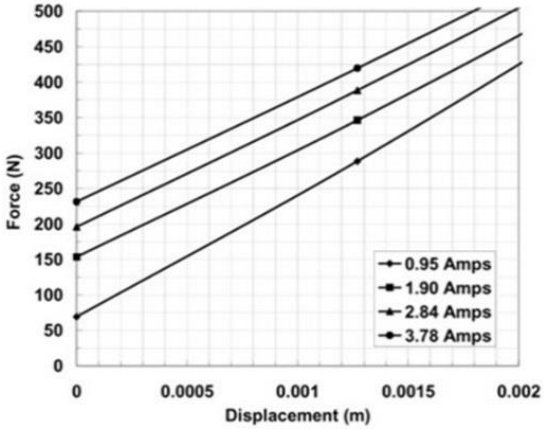

Figure 5) The force vs. displacement diagram.

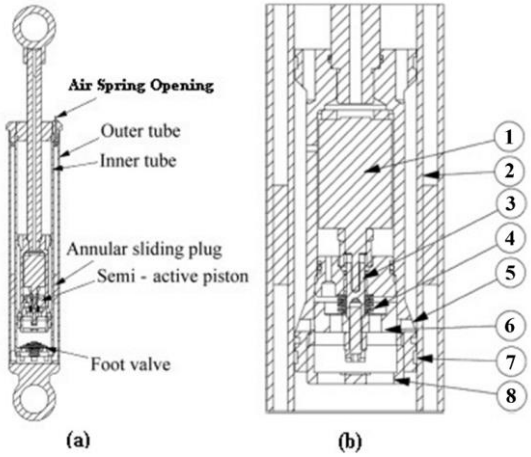

Figure 6) The MR damper details with air spring.

Then, the fluid runs form the outer edge of the disc 6, and radially goes from eight holes 5 to the space 2. The ring 7 do not allow the fluid to bypass the valve. Next, the fluid goes to the extension case. The valve disc is located on the valve shaft 3. The fluid is separated from the solenoid 1 by sealing the shaft and the valve is closed by the solenoid. The valve spring 4 is located on the valve shaft help the solenoid to close the valve. According to the presented structure, the required MR-fluid is roughly 0.3 liters that is less than the previous types; therefore, it leads to low cost of manufacturing.

The air spring piston is installed on the upper end of the MR damper and it fixes the rod guide of the MR damper. It performs the function of the piston that changes the volume and pressure of the cylinder tube and at the same time, it carries out the role of sealing, which maintains pressure by preventing the internal nitrogen gas from leaking. The inner tube changes the spring load (calculated previously by linear spring model) by changing the volume and plays the role of the accumulator together with the outer tube. The inner tube and outer tube have different lengths but other dimensions are all the same. To integrate the rolling-lobe-type air spring with the MR damper, first, the existing air spring's stroke was checked and designed. To calculate the internal pressure intensity, a static structure is analyzed for the conceptually designed dimensions. Table 2 shows the cylinder tube's dimensions and material properties used for the analysis. The characteristic of new air spring is shown in Figure. 8.

Table 2) Dimensions and material properties of the cylinder tube

Description	Value
O/Tube Diameter	38 mm
O/Tube Thickness	3 mm
I/Tube Diameter	25 mm
I/Tube Thickness	2.5 mm
Yield Strength	320 MPa

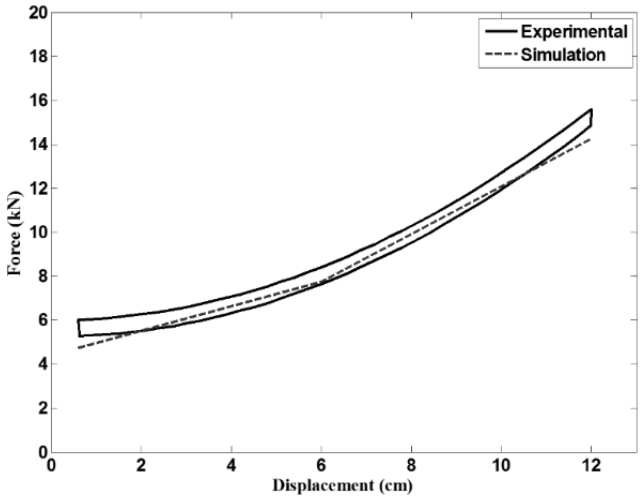

Figure 7) Characteristic of new air spring

The nonlinear characteristic of air spring that is shown in Figure. 7 is obtained after manufacturing, but in mathematical calculations, linear characteristics were used (according to Eq. 9). The results show that there is a good agreement between the test results and the developed mathematical model. A test bench (see Figure. 8) was designed for characterizing the prototyped MR damper. The test bed set up used for measuring the damper's transferred force in various velocity ranges and for various input currents.

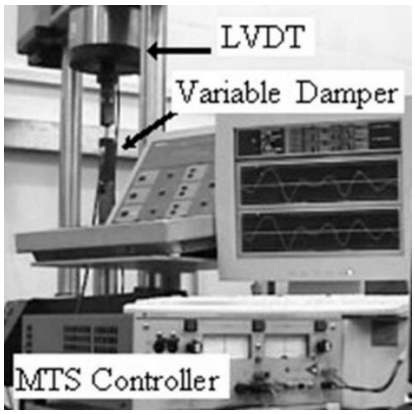

Figure 8) Test design of prototyped MR damper.

Open length of damper is 200 mm and its diameter is 40 mm. In comparison with one of commercial MR damper in the market (i.e. RD 8040-1 that is made by LORD corporation), it shows that both dimensions of the fabricated damper are smaller.

According to graph, the maximum load due to the air spring was ~16 kN. This satisfies the maximum load conditions of the existing air spring. A selected electrical field value is kept during a typical characterization trial [14]. The test is done for four different currents (0, 0.5, 1.0 and 1.5 ampere). The agreements between all the cycles for manufactured damper's parameters were very good. The results for one cycle of damping force vs. velocity are shown in Figure. 9.

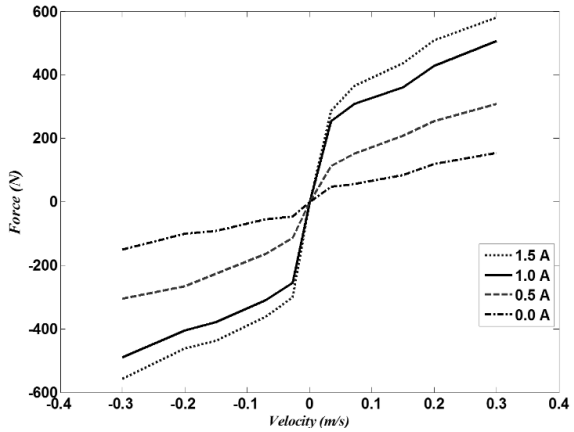

Figure 9) Force-velocity diagram of new MR damper.

The results indicate that the damping force following the durability test increased slightly. They are acceptable in comparison with required forces for passenger car simulated and modeled by Zareh et al. [3]. An increase in the damping force seems to have been caused by the change in the MR fluid viscosity. Offset at origin is due to gas pre-charge required for temperature compensation [15,16]. To show if the oil leakage following the durability test, the sample was checked and compared in terms of the weights prior to and following the test. The results revealed that maximum change was 0.30% that meets the desired. To examine the fabricated MR damper, it was conducted with the exciting velocity of 1 mm/s, stroke length of ±12 mm and a fixed frequency of 1.67Hz. The test is performed for six cycles for zero ampere (A), 0.5A, 1.0A and 1.5 A. The agreement between all the cycle hysteresis curves for manufactured damper's parameters is very good. The results for one cycle are shown in Figure. 10.

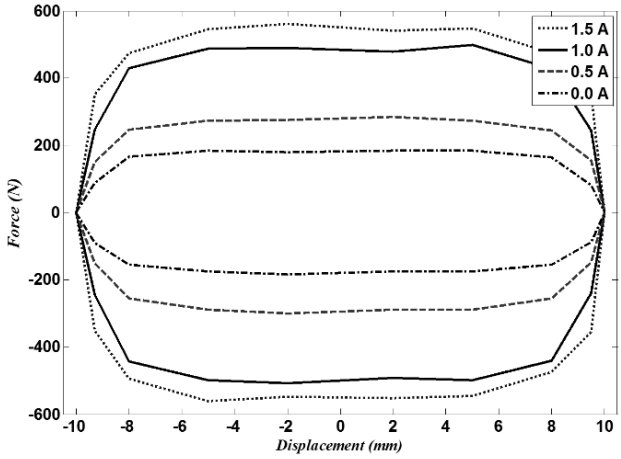

Figure 10) Force-displacement diagram of new MR damper.

As the results in Figure. 10 show, the maximum load roughly is ~600N. This satisfies the maximum load conditions of the new air spring and the oscillations are very good showing that it can be implemented on real passenger cars.

4. Experimental test bed

The MR dampers have been manufactured in this study are added parallel with the passive dampers to set the suspension. A state observer is necessary to estimate known states. A Kalman filter has been designed for our

purpose [3]. Moreover, data acquisition card for controlling the speed, a computer to record the experimental data, accelerometer for measuring road displacement, wheel displacement, and vehicle body displacement, tachometer for measuring wheel speeds, MTS-407 and a power converter are used as elements of controller on board. The two steps are used as implemented control strategy.

Calculating of desired control force using of an optimal controller as first stage. In the second step, regulates the input current to the dampers based on the desired forces (here the Bingham modified model is used). Figure 11 shows the proposed control strategy.

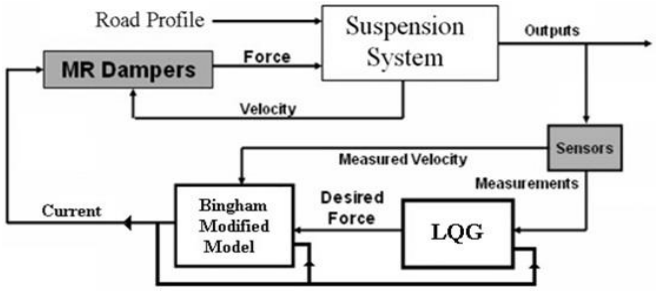

Figure 11) Control strategy block diagram.

Here, accelerators on wheel hub and seat are measuring corresponded accelerations. Then, these values are sent to the LQG to determine appropriate forces. After that, required currents are calculated by forces obtained by LQG (by Bingham modified model). The manufactured MR damper on the test vehicle is shown in Figure. 12.

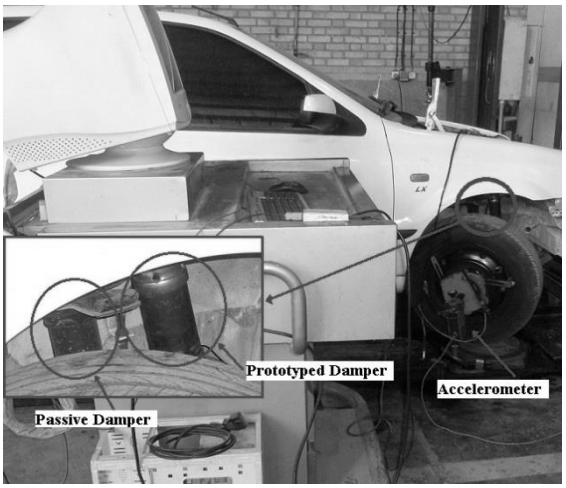

Figure 12) Location of the MR damper on the vehicle.

Here, accelerators on wheel hub and seat are measuring corresponded accelerations. Then, these values are sent to the LQG to determine appropriate forces simulated by MATLAB. After that, required currents are calculated by forces obtained by LQG by means of Bingham modified model. Currents are converted to the voltages and sent to the MR damper.

The suspension is excited through a shaker with consider road profile and the sampling data is recorded by 1000 Hz [19, 20]. As mentioned earlier, in this paper, the Bingham modified model [11], [12], which is modeled as having a friction component augmented by a Newtonian viscosity component is used. This model

simulated by MATLAB and is connected to MTS controller and LQG for calculating the required currents. The relation between force and displacement for the MR actuators is expressed by:

$$f_d = \frac{12\eta L A_p^2}{\pi D D_h^3}\dot{u}(t) + \frac{3L\tau_y}{D_h}A_p \,\mathrm{sgn}[\dot{u}(t)] \tag{12}$$

where L is the length of the piston, A_p is the cross sectional area of the piston, η is the Newtonian viscosity, independent of the applied magnetic field. D is the inner diameter of the vat, D_h is the diameter of the small gap in the piston, and u(t) is the relative displacement of the piston. The shear stress τ_y as function of input current I is expressed by:

$$\tau_y = A_1 e^{-I} + A_2 \ln(I + e) + A_3 I \tag{13}$$

The numerical value of MR damper's parameters and MR fluid for obtaining the current are shown in Table 3 and 4, respectively. These values are obtained by trial and error to achieve desire responses.

Table 3) Numerical values of MR damper

L (m)	A_p (m^2)	D (m)	D_h (m)
0.055	0.00215	0.0236	0.002

Table 4) Numerical values of MR fluid

η (Pa-s)	A_1	A_2	A_3
0.9	-1363	1496	112

5. Results

One of the desired points of current article is to reduce the oscillations of passengers using the fabricated MR dampers during road excitation. Therefore, the effect of Bingham modified model and solenoid with the prototyped MR damper are simulated under road excitation. The bumper excitation as road surface is compatibly generated using a bumper with 7 cm high, 4 cm wide with sum of the road profile by Eq. (14). For experimental road profile a shaker is used.

Responses of the passenger (front-right seat) due to the road profile excitation with constant velocity 75 km/h are shown in Figures. 13-14. The test also performed for different speeds like 30 and 60 km/h. Here, only the results corresponded to the 75 km/h are presented.

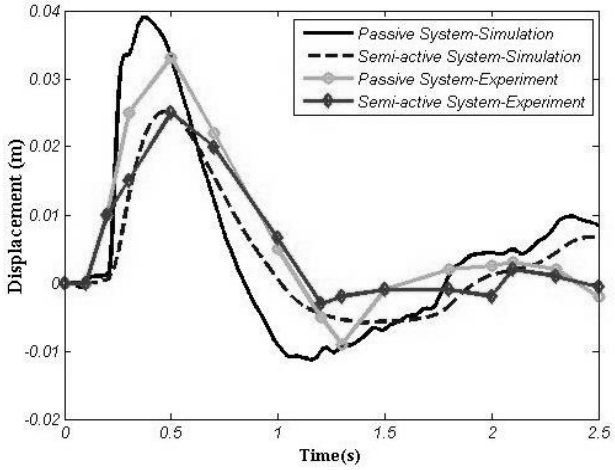

Figure 13) Displacement of front right seat.

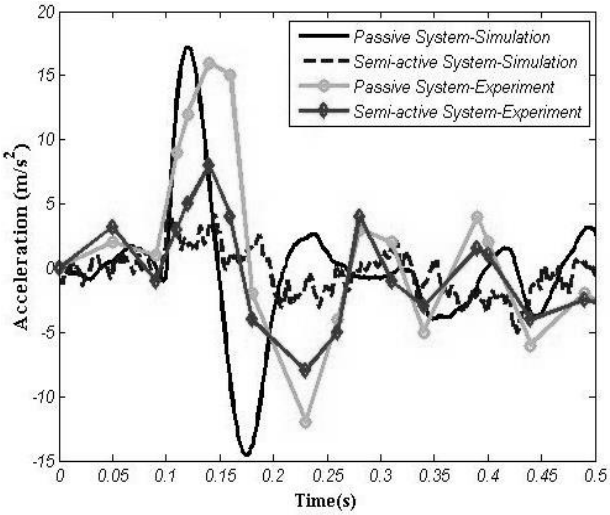

Figure 14) Acceleration of front right seat.

The graphs show how the controlled system behaves under the road excitation. In addition, as depicted, it is possible to achieve comfort driving by reducing the amplitude of the displacement and acceleration. Figure 15 shows the road holding for front right wheel.

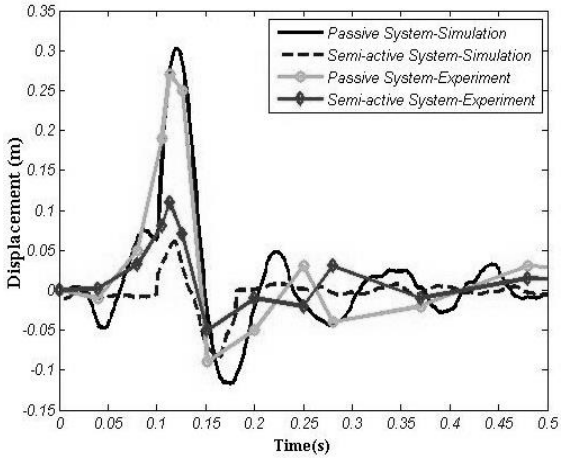

Figure 15) Road holding for front right wheel.

According to the Figure, the dampers could reduce the vibration of the wheel [13,16], which leads to increased road holding. Road holding promotion leads to better stability [3]. The required force to reach the system to the desired responses is presented in Figure. 16.

As can be seen, the maximum generated force during the excitation is in the range of damping force of the fabricated MR damper. All in all, based on the presented results, the performance of the fabricated damper is acceptable.

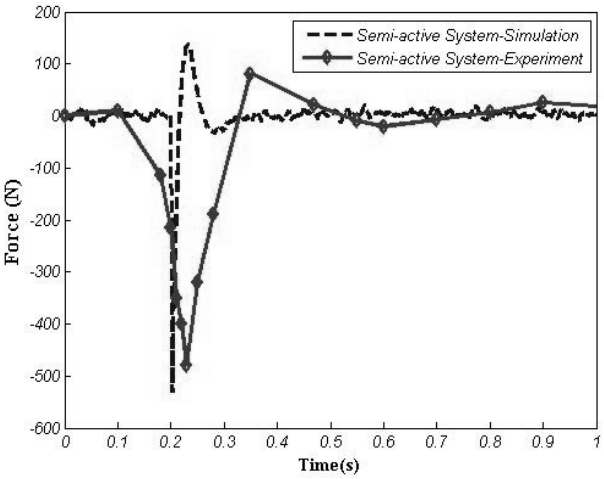

Figure 16) Generated force by front right damper.

6. Conclusion

This study, first, presented a new type of MR damper with internal solenoid, which is integrated with the air spring. The forces generated by the semi-active damper are measured, its durability is tested, which was 0.30% that satisfies the test criteria. After that, the fabricated MR dampers are applied on the real vehicle. The manufactured dampers are added to the suspension system parallel to the passive dampers. The vehicle is excited by a bumper to check the performance of the MR dampers. As illustrated by results, they could reduce the oscillation of the seats and road holding which led to comfort driving and stability. There was a good agreement between the experimental and simulation results. The results showed the performance of the MR dampers is acceptable under the excitation.

References

[1]Parabakar, R. S., Sujatha, C. and Narayanan, S., "Optimal Semi-Active Preview Control Response of a Half Car Vehicle Model with Magneto-rheological Damper," Journal of Sound and Vibration, 2009, 326, 400-420.

[2]Yahaya, M. S. and Osman, J., "Modeling and Control of The Active Suspension System Using Proportional Integral Sliding Mode Approach," Asian Journal of Control, 2005, 7, 91-98.

[3]Zareh, S. H., Sarrafan, A., Khayyat, A. A. A. and Zabihollah, A., "Intelligent Semi-Active Vibration Control of Eleven Degrees of Freedom Suspension System Using Magnetorheological Dampers," Journal of Mechanical Science and Technology, 2012, 26, 323-334.

[4]Dong, X. M., Yu, M., Liao, C., Chen, W. and Li, Z., "Rapid Control Prototyping Development of Intelligent Control System of Vehicle Semi-Active Suspension," Proceedings of 7th World Congress on Intelligent Control and Automation, Chongqing, China (June 25-27, 2008).

[5]Nell, S. and Steyn, J. L., "Experimental Evaluaiton of an Unsophisticated Two State Semi-Active Damper," Journal of Terramechanics, 1994, 31, 227-238.

[6]Elmer, K. F. and Gentle, C. R., "A Parsimonious Model for the Proportional Control Valve," Proceedings of the Institution of Mech. Engineers, Part C: J. of Mechanical Engineering Science, 2001, 215, 1357–1363.

[7]Jazar, G. N. and Golnaraghi, F., "Engine Mounts For Automotive Application," Shock and Vibration Digest, 2002, 34, 363-379.

[8]Eslaminasab, N., Gillespie, T., Khamesee, B. and Golnaraghi, F., "Modeling And Testing of An In-House Prototype Twin-Tube Semi-Active Damper," International Journal of Heavy Vehicle Systems, 2009, 16, 431-458.

[9]Zapateiro, M., Pozo, F., Karimi, H. R. and Luo, N., "Semi-Active Control Methodologies For Suspension Control With Magnetorheological Dampers," IEEE/ASME Transactions on Mechatronics, 2012, 17, 370-380.

[10]Zareh, S. H., Sarrafan, A. and Khayyat, A. A. A., "Clipped Optimal Control of 11-DOFs of a Passenger Car Using Magnetorheological Damper," Proceedings of IEEE International Conference on Computer Control and Automation, Jeju Island, Korea (May 1-3, 2011).

[11] Xu, Z. D. and Guo, Y. Q., "Neuro Fuzzy Control Strategy for Earthquake Excited Nonlinear Magnetorheological Structures," Soil Dynamics and Earthquake Engineering, 2008, 28, 717-727.

[12] Zareh, S. H., Fellahjahromi, A., Hayeri, R., Khayyat, A. A. A., and Zabihollah, A., "LQR and Fuzzy Controller Application with Bingham Modified Model in Semi-Active Vibration Control of 11-DOFs Full Car Suspension System," International Journal on Computing, 2011, 1, 39-44.

[13] Huang, Z. S., Wu, C. and Hsu, D. S., "Semi-Active Fuzzy Control of MR Damper on Structures by Genetic Algorithm," Journal of Mechanics, 2009, 25, 1-6.

[14] Sayyaadi, H. and Zareh, S. H., "Intelligent Control of An MR Prosthesis Knee Using of A Hybrid Self-Organizing Fuzzy Controller And Multidimensional Wavelet NN," Journal of Mechanical Science and Technology, 2017, 31, 3509-3518.

[15] Paciello, V. and Pietrosanto, A., "Magnetorheological Dampers: A New Approach of Characterization," IEEE Transactions on Instrumentation and Measurement, 2011, 60, 1718-1723.

[16] Peng, Y. B., Zhang, Z. K., Yang J. G. and Wang, L. H., "Full-Scale Simulations of Magnetorheological Damper for Implementation of Semi-Actively Structural Control, Journal of Mechanics, 2019, 35, 549-562.

[17] McCloy, D. and Martin, H., Control of Fluid Power: Analysis and Design, Ellis Horwood Limited, 2nd ed, 1980.

[18] Ryff, P. F., Electric Machinery, Prentice-Hall, New Jersey, 1994.

[19] Case, D., Taheri, B. and Richer, E., "Design and Characterization of A Small-Scale Magnetorheological Damper for Tremor Suppression," IEEE/ASME Transactions on Mechatronics, 2011, 99, 1-8.

[20] Roumy, J. G., Boulet, B. and Dionne, D., "Active Control of Vibrations Transmitted Through A Car Suspension," International Journal of Vehicle Autonomous Systems, 2004, 2, 236-254.